The pretranslocation ribosome is targeted by GTP-bound EF-G in partially activated form

Vasili Hauryliuk*†, Vladimir A. Mitkevich‡§, Natalia A. Eliseeva‡, Irina Yu. Petrushanko‡, Måns Ehrenberg*¶, and Alexander A. Makarov‡

*Department of Cell and Molecular Biology, Molecular Biology Program, Uppsala University, S-75 124 Uppsala, Sweden; †Institute of Technology, University of Tartu, Nooruse Street 1, Room 425, 50411 Tartu, Estonia; ‡Engelhardt Institute of Molecular Biology, Russian Academy of Sciences, Vavilov Street 32, Moscow 119991, Russia; and §Centre for Medical Studies in Russia, University of Oslo, Vavilov Street 34/5, Moscow 119334, Russia

Communicated by Joachim Frank, New York State Department of Health, Albany, NY, August 18, 2008 (received for review July 17, 2008)

Translocation of the tRNA·mRNA complex through the bacterial ribosome is driven by the multidomain guanosine triphosphatase elongation factor G (EF-G). We have used isothermal titration calorimetry to characterize the binding of GDP and GTP to free EF-G at 4°C, 20°C, and 37°C. The binding affinity of EF-G is higher to GDP than to GTP at 4°C, but lower at 37°C. The binding enthalpy and entropy change little with temperature in the case of GDP binding but change greatly in the case of GTP binding. These observations are compatible with a large decrease in the solvent-accessible hydrophobic surface area of EF-G on GTP, but not GDP, binding. The explanation we propose is the locking of the switch 1 and switch 2 peptide loops in the G domain of EF-G to the γ-phosphate of GTP. From these data, in conjunction with previously reported structural data on guanine nucleotide-bound EF-G, we suggest that EF-G enters the pretranslocation ribosome as an ''activity chimera,'' with the G domain activated by the presence of GTP but the overall factor conformation in the inactive form typical of a GDP-bound multidomain guanosine triphosphatase. We propose that the active overall conformation of EF-G is attained only in complex with the ribosome in its ''ratcheted state,'' with hybrid tRNA binding sites.

GTPase | guanine nucleotide binding | isothermal titration calorimetry | thermodynamic parameters of interaction

In all organisms, the ribosomal protein elongation cycle is facilitated by two guanosine triphosphatases (GTPases). The first, called elongation factor Tu (EF-Tu) in bacteria and elongation factor 1A in eukaryotes, makes the delivery of aminoacyl-tRNAs to the mRNA-programmed ribosome rapid and accurate. The second, called elongation factor G (EF-G) in bacteria and elongation factor 2 in eukaryotes, makes translocation rapid and accurate. In translocation, mRNA is moved one codon in the ribosomal frame, peptidyl-tRNA is moved from the acceptor site to the peptidyl (P) site, and deacylated tRNA is moved from the P site to the exit (E) site (1). EF-Tu is a three-domain GTPase (2), whereas EF-G has five domains (3, 4). Both factors appear to undergo large conformational changes during their cycles, with distinct active GTP-bound (*T*) and inactive GDP-bound (*D*) conformations (1) driven by the exchange of GDP for GTP or the conversion of GTP to GDP by hydrolysis. These exchange reactions take place in their G domains (2, 5, 6), which contain the mobile peptide loops switch 1 and switch 2 conserved in all GTPases (7). In a GDP-bound GTPase, these loops are often disordered and highly mobile, whereas in a GTP-bound GTPase, they are often ordered and locked to the γ-phosphate of GTP (7). Accordingly, it is the local conformational switches of the G domain of multidomain GTPases that drive the conformational changes between their *D* and *T* forms (7, 8).

These general features are clearly seen by the distinct overall conformations of the crystal structures of free EF-Tu in complex with GDP (9) and in complex with the nonhydrolyzable GTP analogue GDPNP (2). In the case of EF-Tu, therefore, the free factor assumes the *T* conformation when GDP is exchanged for GTP, and the *T* form is further stabilized by the presence of aminoacyl-tRNA in ''ternary complex'' with EF-Tu·GTP (10).

However, in the case of EF-G, the conformational switching has remained a riddle. It was long believed that EF-G is in the active GTP-bound *T* conformation as it enters the pretranslocation ribosome and that EF-G changes conformation to the *D* form after completed translocation, leading to rapid dissociation of the factor from the ribosome (11). More recently, Rodnina *et al.* (12) disproved the ''classic'' translocation model, showing that GTP hydrolysis on EF-G occurs rapidly and before completion of translocation. From this, they suggested that EF-G operates as an ATP-driven motor protein, where the power stroke often occurs after, and not before, hydrolysis of ATP (13). The assumption still was that EF-G enters the ribosome in the GTP-bound *T* form, distinct from the *D* form of the factor. This view was challenged by Ehrenberg and coworkers (14), arguing from nitrocellulose binding experiments that the affinity of GTP to EF-G is much smaller than that of GDP, such that in the living cell, EF-G is likely to enter the pretranslocation ribosome in the *D* form in complex with GDP and that GDP-to-GTP exchange occurs on the ribosome-bound factor. These results were soon to be questioned by Rodnina and coworkers (15), demonstrating with fluorescence methods that the affinities of GDP and GTP to free EF-G are very similar and, hence, that the pretranslocation ribosome is targeted by GTP-bound free EF-G (15).

In 1994, two groups independently reported crystal structures of the GDP-bound *D* form of EF-G (4, 16), along with a similar structure of the apo-form of the factor (3). The GTP-bound form of free EF-G was subsequently studied by small-angle x-ray scattering (SAXS) and found to be indistinguishable from the crystal *D* form, as judged from radii of gyration and length distributions (17). A ribosome-bound *T* form of EF-G, structurally distinct from the free *D* form of the factor, was, however, identified with cryoelectron microscopy (cryo-EM) (ref. 1 and references therein). In these cryo-EM structures, domains III, IV, and V are oriented differently from domains I, II, and G′ than in the crystal structures of GDP-bound EF-G (3, 17). After a long search, the crystal structure of an EF-G mutant in complex with the GTP analogue GDPNP was solved (18) and found to be similar to the GDP-bound crystal structures of EF-G in the *D* form and distinct from the cryo-EM structures of ribosome-bound EF-G in the *T* form. To explain these and other structural observations, the thermodynamic conditions for those conformational switches of GTPases, which are conditional on

Author contributions: V.H., V.A.M., and I.Y.P. designed research; V.H., V.A.M., N.A.E., and I.Y.P. performed research; V.H., V.A.M., I.Y.P., and M.E. analyzed data; and V.H., V.A.M., M.E., and A.A.M. wrote the paper.

The authors declare no conflict of interest.

¶To whom correspondence should be addressed. E-mail: ehrenberg@xray.bmc.uu.se.

This article contains supporting information online at www.pnas.org/cgi/content/full/0807912105/DCSupplemental.

Table 1. Thermodynamic parameters of EF-G binding to GDP and GTP determined by ITC*

Sample	Ligand	T, °C	K_a,† M^{-1}	K_d,‡ μM	ΔH^0,§ kcal/mol	$T\Delta S^0$,¶ kcal/mol	ΔG^0,‖ kcal/mol
EF-G	GDP	4	1.4×10^5	7.1	−5.61	0.93	−6.54
	GDP	25	1.1×10^5	9.1	−5.90	0.96	−6.86
	GDP	37	6.0×10^4	16.7	−6.31	0.47	−6.78
	GTP	4	2.8×10^4	35.7	3.74	9.40	−5.66
	GTP	25	1.2×10^5	8.3	−1.70	5.25	−6.95
	GTP	37	1.1×10^5	9.1	−5.14	2.00	−7.14
EFG·GTP**	GDP	4	1.8×10^5	5.6			−6.66
EFG·GTP**	GDP	37	6.2×10^4	16.1			−6.80
EFG·GDP**	GTP	4	3.2×10^4	31.2			−5.71
EFG·GDP**	GTP	37	9.1×10^4	11.0			−7.03

*All measurements were performed two to four times in phosphate buffer (5 mM K_2HPO_4, 10% glycerol, 1 mM DTT, 95 mM KCl, and 5 mM $MgCl_2$, pH 7.5).
†K_a, affinity constant; standard deviation did not exceed ± 20%.
‡K_d, dissociation constant; calculated as $1/K_a$.
§ΔH^0, enthalpy variation; standard deviation did not exceed ±10%.
¶$T\Delta S^0$, entropy variation; calculated from the equation $\Delta G^0 = \Delta H^0 - T\Delta S^0$.
‖ΔG^0, Gibbs energy; calculated from the equation $\Delta G^0 = -RTlnK_a$.
**The model of competitive ligand binding was used (see *Materials and Methods* and ref. 22).

the presence of auxiliary ligands or the target molecular complex, were described (19).

In this work, we have used isothermal titration calorimetry (ITC) to estimate the equilibrium constants, along with the enthalpic and entropic components for GDP and GTP binding to EF-G at different temperatures. Our data address the apparent discrepancy between previous reports (14, 15) on the relative binding affinities of GDP and GTP to EF-G. Furthermore, we demonstrate that GTP, but not GDP, binding to free EF-G generates a conformational change of the factor, which is compatible with the movement of ≈15 hydrophobic amino acid residues from a solvent exposed to a solvent-protected state. We propose that this structural change is caused by the locking of the switch 1 and switch 2 peptide loops in the G domain of EF-G to the γ-phosphate of GTP, thereby reducing the exposed hydrophobic surface area of the factor. Such a local conformational change of the G domain of EF-G is, we suggest, responsible for the change in Trp fluorescence observed on GTP binding, but not GDP binding, to the factor (15).

From the present observations, the structural observations summarized above, and further development [see supporting information (SI) *Appendix*, section 1.2] of our recently published theory on conditional conformational switching of GTPases (19), we propose that EF-G enters the pretranslocation ribosome as an "activity chimera," with the G domain activated but the overall protein conformation in the inactive *D* form. The active overall conformation of EF-G is, we suggest, only attained in complex with the ribosome in its "ratcheted state," with hybrid tRNA binding sites.

With this novel scenario as a starting point, we also propose explanations for why crystal structures of EF-G in complex with GTP or one of its analogues have been hard to come by and why GDPNP- and GDPCP-bound structures in the *D* form only exist for a mutant of EF-G with reduced affinity to these GTP analogues.

Results

Affinities of GDP and GTP to EF-G at Different Temperatures. There are conflicting data in the literature regarding the relative affinities of GDP and GTP to free EF-G as estimated from nitrocellulose filter binding (14) and stopped flow with fluorescence detection (15). Here, we have used ITC to remeasure these affinities at 4°C, 25°C, and 37°C, and the results are summarized in Table 1 as association (K_a) and dissociation (K_d) equilibrium constants. The binding stoichiometry in phosphate buffer always reflected a 1:1 stoichiometry between EF-G and guanine nucleotide. When the buffer was changed to Tris, the activity of EF-G was reduced but the binding constants remained unaltered (data not shown). A typical set of ITC data for GDP and GTP binding to EF-G in the phosphate buffer at 4°C and 37°C is shown in Fig. 1. The top panels present the raw calorimetric data for the ligand-into-protein titration, and the bottom panels present the binding isotherms. The binding curves were fitted assuming one set of sites. The K_a-value for GDP binding decreased more than twofold when the temperature increased from 4°C ($K_a = 1.4 \times 10^5$ M^{-1}) to 37°C ($K_a = 6.0 \times 10^4$ M^{-1}), and the K_a-value at 25°C was intermediate ($K_a = 1.1 \times 10^5$ M^{-1}). The K_a-value for GTP binding to EF-G, in contrast, increased more than fourfold when the temperature increased from 4°C ($K_a = 2.8 \times 10^4$ M^{-1}) to 25°C ($K_a = 1.2 \times 10^5$ M^{-1}), after which the K_a-value change with temperature was small ($K_a = 1.1 \times 10^5$ M^{-1} at 37°C). Accordingly, the affinity of EF-G to GDP was fivefold higher than to GTP at 4°C, but at 37°C, the affinity to GDP was twofold lower than to GTP. Overall, these results are consistent with earlier estimates of the affinities of EF-G to GDP and GTP (15, 21, 22); in particular, in qualitative agreement with data from Rodnina and coworkers (15), the K_a-values for GDP and GTP binding to EF-G at 37°C were estimated as 2.0×10^4 M^{-1} and 4.0×10^4 M^{-1}, respectively. In conclusion, the ITC data confirm that at 37°C, the affinity of free EF-G is slightly higher to GTP than to GDP, in accordance with the data from Rodnina and coworkers (15) and in contrast to our previous report (14). The latter included a cooling step on ice before nitrocellulose filter binding, meaning that the measurement reflected the 0°C condition, where GTP is likely to have lower affinity to EF-G than GDP (Table 1), and not the intended 37°C condition.

As a control, the current binding experiments were complemented by "displacement titrations" (23), where GDP was chased from the EF-G·GDP binary complex by GTP and *vice versa*. The equilibrium constants for guanine nucleotide binding to EF-G were estimated from a competitive ligand binding model (23), and the parameter estimates obtained with phosphate buffer at 4°C and 37°C were virtually the same as those obtained by the direct method under the same condition (Table 1).

Energetics of EF-G·GDP and EF-G·GTP Complex Formation. The association equilibrium constant (K_a) estimates described in the previous section (Table 1) provided information on the standard

BIOCHEMISTRY

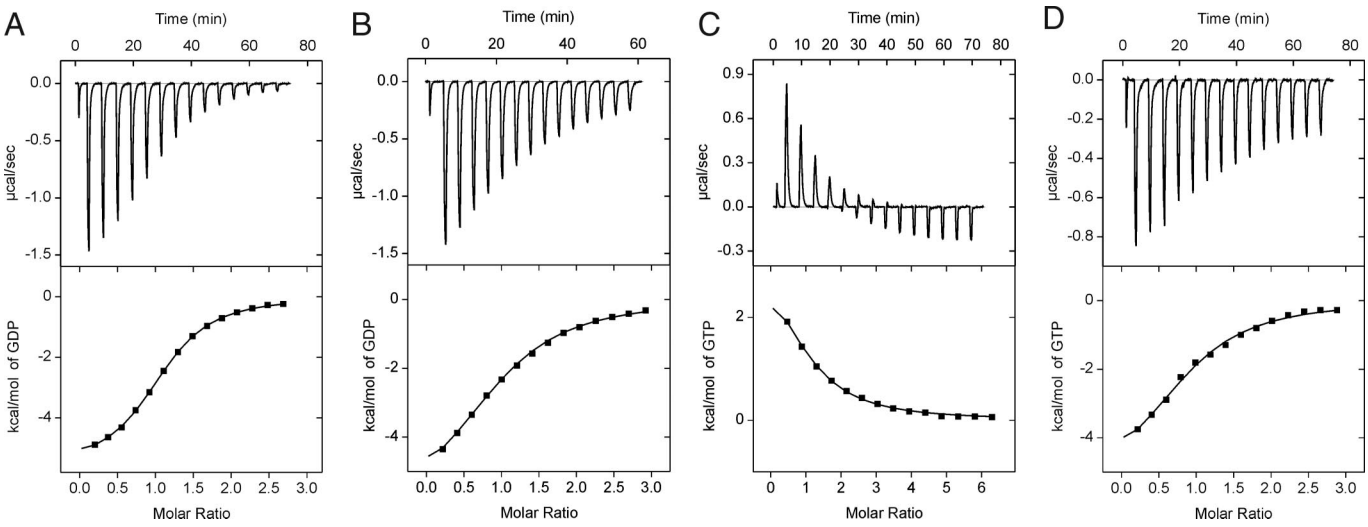

Fig. 1. ITC titration curves (Upper) and binding isotherms (Lower) for EF-G interaction with GDP at 4°C (*A*) and 37°C (*B*) and with GTP at 4°C (*C*) and 37°C (*D*) in phosphate buffer (pH 7.5).

free energy change ($\Delta G^0 = G_C^0 - G_F^0$) when EF-G and GDP or GTP were brought from their free state with standard free energy G_F^0 to their bound state with standard free energy G_C^0 through $K_a = e^{-\Delta G^0}/RT$. R is the gas constant [kcal/(mol·K)], and T is the absolute temperature (K). In addition, the ITC method provided direct information on the corresponding enthalpy change ($\Delta H^0 = H_C^0 - H_F^0$), because EF-G formed a complex with GDP or GTP. The direct readout measured is the heat that must be added (positive ΔH^0) or removed (negative ΔH^0) to keep the temperature unchanged (isothermal) on complex formation. This is illustrated in Fig. 1, showing experiments on EF-G binding to GDP at 4°C (Fig. 1*A*) and 37°C (Fig. 1*B*) as well as to GTP at 4°C (Fig. 1*C*) and 37°C (Fig. 1*D*). In panels *A*, *B*, and *D*, heat was removed (ΔH^0-negative), but in panel *C*, heat was supplied (ΔH^0-positive) to maintain the isothermal condition during the ligand titrations.

Since the change of Gibbs standard free energy (ΔG^0) is related to the change of standard enthalpy (ΔH^0) and entropy (ΔS^0) through $\Delta G^0 = \Delta H^0 - T\Delta S^0$, knowledge of ΔG^0 and ΔH^0 of the studied reactions also allowed estimation of their standard entropy change, ΔS^0, on complex formation. The ΔG^0, ΔH^0, and ΔS^0 values for GDP and GTP binding to EF-G at 4°C, 25°C, and 37°C are summarized in Table 1. In the case of GDP, ΔH^0 was −5.6 kcal/mol at 4°C and decreased slightly further to −6.3 kcal/mol at 37°C. The entropy contribution, $T\Delta S^0$, to the reaction was small and positive (i.e., the complex formation led to an entropy increase with little temperature variation) (Table 1 and Fig. 2*B*). In the case of GTP, ΔH^0 was +3.74 kcal/mol at 4°C, decreased to −1.70 kcal/mol when the temperature was increased to 25°C, and decreased further to −5.14 kcal/mol when the temperature was further increased to 37°C. The entropy change attributable to complex formation was positive and remarkably large at 4°C, with a $T\Delta S^0$ value of 9.2 kcal/mol. As the temperature increased, $T\Delta S^0$ remained positive but decreased to 5.25 kcal/mol at 25°C and further to 2.0 kcal/mol at 37°C.

When ΔH^0 was plotted against temperature in the GDP and GTP cases, straight lines with negative slopes were obtained (Fig. 2*A*). From these, we estimated the change in the heat capacity, $\Delta C_p = d(\Delta H)/dT$, on complex formation as −20 cal·mol^{-1}·K^{-1} in the case of GDP and −270 cal·mol^{-1}·K^{-1} in the case of GTP. In both cases, ΔC_p was virtually constant, meaning that a plot of ΔS^0 against the logarithm of the temperature should give a straight line with ΔC_p as the slope according to the integrated van't Hoff equation (24). Consistent with this, such plots gave straight lines in the GDP and GTP cases, with similar estimates of ΔC_p (Fig. 2*B*) as from the enthalpy plots (Fig. 2*A*). The large decrease in heat capacity on complex formation between EF-G and GTP, but not GDP, suggests that GTP binding to EF-G significantly decreased the solvent-exposed

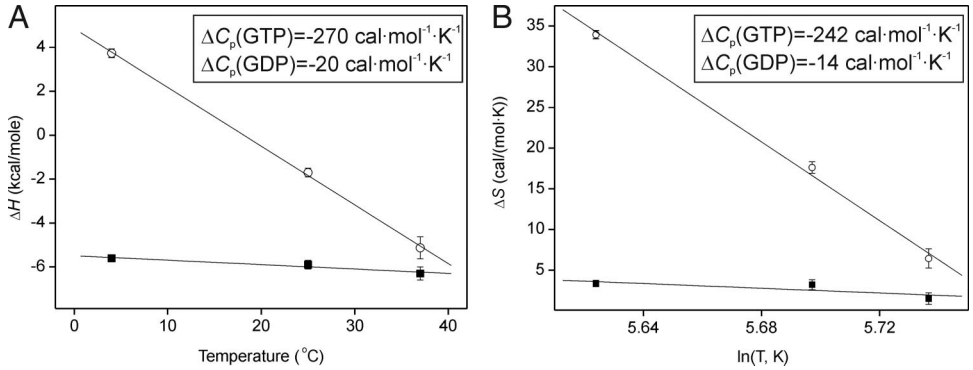

Fig. 2. Temperature dependence of entropy and enthalpy of EF-G interactions with GTP and GDP. (*A*) Enthalpy of binding of GDP (filled squares) and GTP (empty circles) to EF-G as a function of the temperature (°C) at pH 7.5. (*B*) Entropy of binding of GDP (filled squares) and GTP (empty circles) to EF-G as functions of the logarithm of the temperature (degrees Kelvin) at pH 7.5. The ΔC_p values obtained from the enthalpy plots are similar to those obtained from the entropy plots.

area of nonpolar amino acids (25). According to Connelly and Thomson (26), transfer of nonpolar residues from a solvent-exposed to a solvent-protected state leads to a ΔC_p decrease corresponding to $0.27\Delta A_{aromatic} + 0.4\Delta A_{nonaromatic}$, where $\Delta A_{aromatic}$ and $\Delta A_{nonaromatic}$ are the protected areas in $Å^2$ attributable to aromatic and nonaromatic amino acids, respectively. From this heuristic formula, we estimated the total decrease in solvent-exposed nonpolar surface area as about 600 $Å^2$. Assuming an area of 30 to 40 $Å^2$ per hydrophobic amino acid residue (27), this would correspond to about 15 aa. This number appears reasonable, since there are more than 15 unresolved hydrophobic amino acid residues in switch-1 of the crystal structure of EF-G·GDPNP (18). To these, one might add some of the resolved residues in switch 1, and more can be found in switch 2.

One possible caveat in this interpretation was putative changes in the pK_a-values of functional groups in protein or ligand on complex formation (25). To study this, we took advantage of the very different ionization enthalpies (ΔH_i) in Tris (11 kcal/mol) and phosphate (1 kcal/mol) buffer (28) by carefully comparing estimated ΔH^0 values for GDP and GTP binding to EF-G in both buffers. We found the ΔH^0 values to be virtually the same in the two buffer systems (not shown), meaning that complex formation was not accompanied by net proton association or dissociation events and, accordingly, that ionization enthalpies were negligible.

Our explanation for the large and negative ΔC_p value on GTP binding as attributable to a reduction of the solvent-exposed hydrophobic surface area gets further support from the previous finding that structural rearrangements in proteins that reduce their hydrophobic surface area are associated with large entropy enhancements in the temperature interval used in our study (29). Indeed, we observed that GTP binding to EF-G was primarily driven by a large entropy increase, particularly at low temperature (Table 1). This phenomenon has been theoretically explained as attributable to the disruption of highly ordered networks of water molecules around hydrophobic amino acids (30), because these become buried in the protein structure. As the temperature increases, the network of solvent molecules becomes less ordered and, hence, the gain in entropy on exclusion of the hydrophobic groups from the aqueous phase decreases and the enthalpic component corresponding to formation of hydrogen bonds increases (30) (Fig. 2).

Discussion

We have used isothermal titration calorimetry to estimate the equilibrium constants as well as the standard enthalpy (ΔH^0) and entropy (ΔS^0) changes for complex formation between GDP or GTP with EF-G at three different temperatures.

In the case of GDP, the guanine nucleotide affinity to the factor is determined by a large enthalpy decrease and a small entropy increase on complex formation. The ΔH^0 and ΔS^0 values change little with temperature, and there is no indication of a conformational change of EF-G as it binds to GDP.

In the case of GTP, there is a large entropy increase on complex formation, which decreases as the temperature increases from 4°C to 37°C (Table 1). The corresponding enthalpy change is positive at 4°C but changes sign and becomes increasingly negative at 25°C and 37°C (Fig. 1 and Table 1). The heat capacity change on complex formation has a numerically large negative value (Fig. 2), which appears constant throughout the temperature interval of our experiments. Our data are qualitatively in line with earlier observations obtained at 25°C for the binding of GDP or GTP to another GTPase, eukaryote release factor 3 in complex with eukaryote release factor 1 (31).

The large entropy increase on GTP binding to EF-G, the decrease of this entropy change with increasing temperature, and the numerically large negative heat capacity change on complex formation all suggest that GTP binding to EF-G induces a conformational change of the factor that brings a hydrophobic surface area, corresponding to about 15 hydrophobic residues, from a solvent-exposed state to a solvent-protected state (see *Results*) (25, 29). This suggests a significant change in the structure of EF-G on GTP binding to the free factor and when GDP is exchanged for GTP. At the same time, a long-standing mystery has been why the free and GDP-bound crystal forms of free EF-G are so similar to the crystal structure of the GDPNP-bound free factor (4, 18, 32) and the SAXS structure of the GTP-bound free factor (17) but distinct from the cryo-EM–derived structure of ribosome-bound EF-G in complex with GDPNP (5, 33). These structural observations suggest, first, that free EF-G does not change its overall conformation from the inactive *D* to the active *T* form when GDP is exchanged for GTP or a GTP analogue and, second, that the active *T* form appears when EF-G is in complex with the ribosome. This suggests that EF-G is a case of "conditional conformational switching" of a GTPase, where the conformational change requires the presence of an auxiliary ligand or the target (19). The occurrence of conformational switching may be summarized by two parameters: the equilibrium relation between the guanine nucleotide free *T* and *D* conformations of the GTPase (equilibrium constant K_0) and the selectivity (ℓ) of GTP binding to the *T* form rather than to the *D* form. When $K_0\ell \ll 1$, there is no switch, but when $K_0\ell \gg 1$, the conformational switch occurs (19). In conditional switching, a ligand or the target (in the case of EF-G, the ribosome) greatly favors the *T* form of the GTPase, making K_0 much larger in the presence than in the absence of the ligand or the target, such that the inequality $K_0\ell \gg 1$ is fulfilled for the ligand or target-bound, but not the isolated, GTPase (19).

On GTP binding, the first step in the switching of a GTPase from the inactive to the active conformation is the locking of the peptide loops switch 1 and switch 2 to the γ-phosphate of GTP (34, 35). In multidomain GTPases, such as EF-G and EF-Tu, it is this local conformational change of the G-domain that subsequently drives the overall *D*-to-*T* transition (8). From this general GTPase scenario in conjunction with our thermodynamic data, we suggest that the decrease in exposed hydrophobic surface area on GTP binding to EF-G is caused by the locking of switch 1 and switch 2 to the γ-phosphate of GTP, bringing these peptide loops from a relatively disordered solvent-exposed (*E*) state to a relatively ordered solvent-protected (*P*) state. At the same time, we propose, that the local *E*-to-*P* transition in the G domain does not suffice to induce the overall *D*-to-*T* transition of EF-G, as explained in SI. Here, we introduce the thermodynamic coupling of a G domain switch from the *E* form to the *P* form to an interdomain global switch from the inactive *D* to the active *T* form. With support from this analysis, we suggest that GTP binds to the *E* form of the G domain with EF-G in the global *D* form and drives the G domain to the *P* form with the factor remaining in the global *D* form. In this scenario, the "effective" association constant, K_A^{GTP}, for GTP binding (19, 36) is approximated by $K_A^{GTP} = Q_{D0}K_{AP}^{GTP}$ (see *SI Appendix*). Here, Q_{D0} is the equilibrium relation between the guanine nucleotide-free *P* and *E* forms of the G domain, given that the overall conformation of the factor is *D*, and K_{AP}^{GTP} is the association constant for GTP binding to the already activated *P* form of the G domain. The overall enthalpy (ΔH^0) and entropy (ΔS^0) changes associated with GTP binding to the free factor are approximated by (*SI Appendix*) $\Delta H^0 = \Delta H_D^0 + \Delta H_{AD}^0$ and $\Delta S^0 = \Delta S_D^0 + \Delta S_{AD}^0$. Here, ΔH_D^0 is the enthalpy change, and ΔS_D^0 is the entropy change to move, in the absence of GTP, switch 1 and switch 2 into positions favorable for subsequent interaction with the γ-phosphate of GTP. Since ΔH_D^0 and ΔS_D^0 are associated with the reduction of a solvent-exposed hydrophobic surface area because of the optimal positioning of switch 1 and switch 2 for binding to the γ-phosphate of GTP,

they are both expected to be numerically large and positive and to decrease with temperature. ΔH^0_{AD} is the enthalpy change and ΔS^0_{AD} is the entropy change when GTP binds to the G domain with switch 1 and switch 2 already in place for interaction with the γ-phosphate of GTP. ΔH^0_{AD} is expected to be numerically large and negative, because of the favorable interaction between the already positioned switch 1 and switch 2 and the γ-phosphate of GTP. In analogy with the entropy change on GDP binding to the G domain, we expect ΔS^0_{AD} to be numerically small and negative. From this qualitative reasoning, we suggest that the large temperature dependence of ΔH^0 and ΔS^0 come from their ΔH^0_D and ΔS^0_D terms, respectively. At low temperature, the positive ΔH^0_D dominates over the negative ΔH^0_{AD} term, but as the temperature increases, ΔH^0_D decreases to the extent that it becomes numerically equal to ΔH^0_{AD}, at which point ΔH^0 changes sign from positive to negative. Since we expect ΔS^0_{AD} to be numerically small, we propose that ΔS^0 is dominated by the ΔS^0_D term.

Despite intensive efforts to obtain crystal structures of EF-G bound to GTP or GTP analogues, it took a long time before Hansson and colleagues (18) managed to obtain the GDPNP structure (18) and, later, the GDPCP (S. Hansson, personal communication) structure. Interestingly, these structures were not obtained for the WT but for a mutant EF-G with reduced affinity to GDPNP (18). The present suggestion that free EF-G in complex with GTP or a GTP analogue is an "activity chimera," with the G-domain activated but the overall structure in the *D* form, may offer an explanation for the difficulty to obtain such crystal structures with WT EF-G. That is, when the overall conformation of EF-G is *D*, this destabilizes the active conformation of the G domain in relation to when the EF-G conformation is *T*, such that switch 1 and switch 2 may undergo fluctuations between their locked and unlocked states (SI). By the same logic, when the G domain is activated, this may induce fluctuations between the *D* and *T* forms of the factor that are absent when the G domain is in the inactive form. It may, we speculate, be such intra- and interdomain fluctuations of EF-G that make formation of stable crystal structures of EF-G bound to GTP or GTP analogues difficult. The mutation that led to crystal structures for the GDPNP-bound (18) and GDPCP-bound (S. Hansson, personal communication) EF-G may, we speculate further, stabilize the *D* form of the factor, thereby attenuating these fluctuations sufficiently so as to allow for the formation of crystal structures suitable for structural analysis.

Recently, Connell *et al.* (5) determined the crystal structure of a GTP-bound divergent EF-G variant from *Thermus thermophilus*, EF-G-2, and made a cryo-EM reconstruction of ribosome-bound native EF-G from the same organism. The overall conformation of free EF-G-2 in complex with GTP was similar to that of ribosome-bound *T. thermophilus* EF-G in complex with GDPNP, as seen by cryo-EM at about 7Å resolution (5) but was distinct from the crystal structure of free EF-G in complex with GDPNP (18). This, we suggest, is because the criterion $K_0\ell \gg 1$ for conformational switching discussed above is fulfilled for free EF-G-2 but not for free native *T. thermophilus* EF-G. We note that switch 1 and switch 2 are well ordered in the GTP-bound structure of free EF-G-2 as well as in the GDPNP-bound EF-G in complex with the ribosome (5), in contrast to the GDPNP-bound crystal structure of free EF-G. This is in line with the prediction that switch 1 and switch 2 fluctuate much less between their locked and unlocked states when the overall conformation of EF-G is *T* compared with when it is *D* (*SI Appendix*).

In the dynamic picture of the solution structure of EF-G that we propose here, the factor enters the pretranslocation ribosome as an "activity chimera," with the G domain preferentially in its activated form with switch 1 and switch 2 locked to the γ-phosphate of GTP, as supported by the present data, whereas the overall structure of the factor is in the inactive *D* form, as supported by crystal structures of EF-G (18) and SAXS observations of GDP- and GTP-bound forms of the factor (17) (Fig. 3). This, we suggest, facilitates rapid association of GTP-bound EF-G by favorable interaction with the GTPase center of the pretranslocation ribosome. Subsequently, the ribosome switches to the ratcheted conformation, with peptidyl-tRNA in the acceptor/P site, deacylated tRNA in the P/E site, and the tRNA originally in the E site ejected (1), concomitantly with a conformational switch of EF-G from the overall *D* form to the overall *T* form (Fig. 3). These coordinated conformational switches of the ribosome and EF-G are, we propose, essential for the triggering of GTP-hydrolysis on EF-G and subsequent completion of the translocation cycle (1).

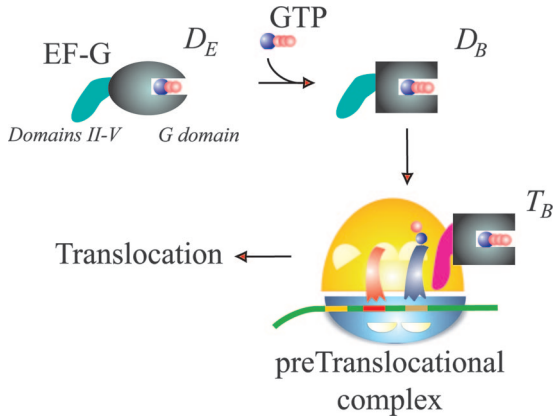

Fig. 3. Model for GTP and ribosome-dependent conformational switching of EF-G. Off the ribosome, GTP binding promotes rearrangements in the G domain of EF-G, corresponding to the locking of switch 1 and switch 2 to the γ-phosphate of GTP ($D_E \rightarrow D_P$ transition). This local transition in the G domain of EF-G does not, however, suffice to promote the global *D*-to-*T* transition of the factor. This occurs concomitantly with the structural change in the pretranslocation ribosome, leading from its relaxed state to its ratcheted state (1), and is rapidly followed by GTP hydrolysis on EF-G and completion of translocation.

Materials and Methods

1. EF-G, GTP, and GDP Preparations. EF-G was overexpressed and purified as described (37), and all guanine nucleotides were purified in a MonoQ column (Amersham Bioscience) as described by Zavialov *et al.* (20).

2. Isothermal Titration Calorimetry. The thermodynamic parameters of EF-G binding to GDP and GTP were measured using a MicroCal VP-ITC instrument as described by Mitkevich *et al.* (31). Experiments were carried out at 4°C, 25°C, and 37°C in phosphate (5 mM K_2HPO_4, 10% glycerol, 1 mM DTT, 95 mM KCl, and 5 mM $MgCl_2$, pH 7.5) or Tris (5 mM Tris-HCl, 1 mM DTT, 95 mM KCl, and 5 mM $MgCl_2$) buffers. Twenty-microliter aliquots of ligands were injected into the 1.42-ml cell containing the EF-G solution to achieve a complete binding isotherm. Protein concentration in the cell ranged from 10 to 60 μM, and ligand concentration in the syringe ranged from 90 to 1000 μM. The heat of dilution was measured by injecting the ligand into the buffer solution or by additional injections of ligand after saturation; the values obtained were subtracted from the heat of reaction to obtain the effective heat of binding. The resulting titration curves were fitted using MicroCal Origin software. Affinity constants (K_a), binding stoichiometry, and enthalpy variations (ΔH) were determined by a nonlinear regression fitting procedure.

The direct binding experiments were complemented by the displacement titration calorimetry method (23) determining an apparent binding constant (K_{app}) corresponding to the displacement of one ligand by another. In this case, EF-G was initially saturated with a ligand L_1 (GDP or GTP) introduced into the calorimeter cell and then titrated with 20-μl aliquots of a ligand L_2 (GTP or GDP). A K_{app}, corresponding to the displacement of L_1 by L_2, was thus determined. Then, knowing the binding constant K_1 of L_1, the value of the binding constant K_2 of L_2 for EF-G was estimated from the equation $K_2 = K_{app}(1+K_1[L_1])$ (23, 31).

ACKNOWLEDGMENTS. We thank Gemma Atkinson for helpful discussions and critical reading of the manuscript. This work was supported by National Institutes of Health Grant RO1 GM070768 and the Swedish Research Council (M.E.), the Molecular and Cellular Biology Program of the Russian Academy of Sciences (A.M.), the Estonian Scientific Fund Grant ETF7616 (to V.H.), and the Russian Fund of National Science (V.M.).

1. Frank J, Gao H, Sengupta J, Gao N, Taylor DJ (2007) The process of mRNA-tRNA translocation. *Proc Natl Acad Sci USA* 104:19671–19678.
2. Kjeldgaard M, Nissen P, Thirup S, Nyborg J (1993) The crystal structure of elongation factor EF-Tu from Thermus aquaticus in the GTP conformation. *Structure* 1:35–50.
3. AEvarsson A, *et al.* (1994) Three-dimensional structure of the ribosomal translocase: Elongation factor G from Thermus thermophilus. *EMBO J* 13:3669–3677.
4. al-Karadaghi S, Aevarsson A, Garber M, Zheltonosova J, Liljas A (1996) The structure of elongation factor G in complex with GDP: Conformational flexibility and nucleotide exchange. *Structure* 4:555–565.
5. Connell SR, *et al.* (2007) Structural basis for interaction of the ribosome with the switch regions of GTP-bound elongation factors. *Mol Cell* 25:751–764.
6. Nissen P, *et al.* (1995) Crystal structure of the ternary complex of Phe-tRNAPhe, EF-Tu, and a GTP analog. *Science* 270:1464–1472.
7. Sprang SR (1997) G protein mechanisms: Insights from structural analysis. *Annu Rev Biochem* 66:639–678.
8. Vale RD (1996) Switches, latches, and amplifiers: Common themes of G proteins and molecular motors. *J Cell Biol* 135:291–302.
9. Polekhina G, *et al.* (1996) Helix unwinding in the effector region of elongation factor EF-Tu-GDP. *Structure* 4:1141–1151.
10. Kaziro Y (1978) The role of guanosine 5′-triphosphate in polypeptide chain elongation. *Biochim Biophys Acta* 505:95–127.
11. Belitsina NV, Glukhova MA, Spirin AS (1975) Translocation in ribosomes by attachment-detachment of elongation factor G without GTP cleavage: Evidence from a column-bound ribosome system. *FEBS Lett* 54:35–38.
12. Rodnina MV, Savelsbergh A, Katunin VI, Wintermeyer W (1997) Hydrolysis of GTP by elongation factor G drives tRNA movement on the ribosome. *Nature* 385:37–41.
13. Sablin EP, Kull FJ, Cooke R, Vale RD, Fletterick RJ (1996) Crystal structure of the motor domain of the kinesin-related motor ncd. *Nature* 380:555–559.
14. Zavialov AV, Hauryliuk VV, Ehrenberg M (2005) Guanine-nucleotide exchange on ribosome-bound elongation factor G initiates the translocation of tRNAs. *J Biol* 4:9.
15. Wilden B, Savelsbergh A, Rodnina MV, Wintermeyer W (2006) Role and timing of GTP binding and hydrolysis during EF-G-dependent tRNA translocation on the ribosome. *Proc Natl Acad Sci USA* 103:13670–13675.
16. Czworkowski J, Wang J, Steitz TA, Moore PB (1994) The crystal structure of elongation factor G complexed with GDP, at 2.7 A resolution. *EMBO J* 13:3661–3668.
17. Czworkowski J, Moore PB (1997) The conformational properties of elongation factor G and the mechanism of translocation. *Biochemistry* 36:10327–10334.
18. Hansson S, Singh R, Gudkov AT, Liljas A, Logan DT (2005) Crystal structure of a mutant elongation factor G trapped with a GTP analogue. *FEBS Lett* 579:4492–4497.
19. Hauryliuk V, Hansson S, Ehrenberg M (2008) Co-factor dependent conformational switching of GTPases. *Biophys J* 95:1704–1715.
20. Zavialov AV, Buckingham RH, Ehrenberg M (2001) A posttermination ribosomal complex is the guanine nucleotide exchange factor for peptide release factor RF3 *Cell* 107:115–124.
21. Arai N, Arai K, Kaziro Y (1977) Further studies on the interaction of the polypeptide chain elongation factor G with guanine nucleotides. *J Biochem* 82:687–694.
22. Baca OG, Rohrbach MS, Bodley JW (1976) Equilibrium measurements of the interactions of guanine nucleotides with Escherichia coli elongation factor G and the ribosome. *Biochemistry* 15:4570–4574.
23. Sigurskjold BW (2000) Exact analysis of competition ligand binding by displacement isothermal titration calorimetry. *Anal Biochem* 277:260–266.
24. Prabhu NV, Sharp KA (2005) Heat capacity in proteins. *Annu Rev Phys Chem* 56:521–548.
25. Jelesarov I, Bosshard HR (1999) Isothermal titration calorimetry and differential scanning calorimetry as complementary tools to investigate the energetics of biomolecular recognition. *J Mol Recognit* 12:3–18.
26. Connelly PR, Thomson JA (1992) Heat capacity changes and hydrophobic interactions in the binding of FK506 and rapamycin to the FK506 binding protein. *Proc Natl Acad Sci USA* 89:4781–4785.
27. Samanta U, Bahadur RP, Chakrabarti P (2002) Quantifying the accessible surface area of protein residues in their local environment. *Protein Engineering* 15:659–667.
28. Pierce MM, Raman CS, Nall BT (1999) Isothermal titration calorimetry of protein-protein interactions. *Methods* 19:213–221.
29. Ladbury JE, Doyle ML (2004) *Biocalorimetry 2*. (John Wiley & Sons, West Sussex, UK), p 259.
30. Finkelstein A, Ptitsyn O (2002) *Protein Physics: A Course of Lectures* (Academic, London).
31. Mitkevich VA, *et al.* (2006) Termination of translation in eukaryotes is mediated by the quaternary eRF1*eRF3*GTP*Mg2+ complex. The biological roles of eRF3 and prokaryotic RF3 are profoundly distinct *Nucleic Acids Res* 34:3947–3954.
32. Laurberg M, *et al.* (2000) Structure of a mutant EF-G reveals domain III and possibly the fusidic acid binding site. *J Mol Biol* 303:593–603.
33. Valle M, *et al.* (2003) Locking and unlocking of ribosomal motions. *Cell* 114:123–134.
34. Bourne HR, Sanders DA, McCormick F (1991) The GTPase superfamily: Conserved structure and molecular mechanism. *Nature* 349:117–127.
35. Sprang SR, Chen Z, Du X (2007) Structural basis of effector regulation and signal termination in heterotrimeric Galpha proteins. *Adv Protein Chem* 74:1–65.
36. Eftink MR, Anusiem AC, Biltonen RL (1983) Enthalpy-entropy compensation and heat capacity changes for protein-ligand interactions: General thermodynamic models and data for the binding of nucleotides to ribonuclease A. *Biochemistry* 22:3884–3896.
37. Antoun A, Pavlov MY, Tenson T, Ehrenberg MM (2004) Ribosome formation from subunits studied by stopped-flow and Rayleigh light scattering. *Biol Proced Online* 6:35–54.